J MATER RES TECHNOL. 2018;xxx(xx):xxx–xxx

Available online at www.sciencedirect.com

jmr&t Journal of Materials Research and Technology

www.jmrt.com.br

Original Article

Properties of manganese ferrite-paraffin composites

Ronaldo Sergio de Biasi[a,*], *Gabriel Burlandy Mota de Melo*[a], *André Ben-Hur da Silva Figueiredo*[a], *Mariella Alzamora Camarena*[b], *José Brant de Campos*[c]

[a] *Seção de Engenharia Mecânica e de Materiais, Instituto Militar de Engenharia, 22290-270 Rio de Janeiro, RJ, Brazil*
[b] *Universidade Federal do Rio de Janeiro, Duque de Caxias, RJ, Brazil*
[c] *Universidade do Estado do Rio de Janeiro, São Cristóvão, RJ, Brazil*

ARTICLE INFO

Article history:
Received 14 June 2017
Accepted 29 September 2017
Available online xxx

Keywords:
Manganese ferrite
Paraffin
Nanoparticles
Composites

ABSTRACT

Manganese ferrite ($MnFe_2O_4$) nanoparticles were dispersed in paraffin and the physical properties of this composite were investigated by X-ray diffraction (XRD), ferromagnetic resonance (FMR), vibrating sample magnetometry (VSM), field cooled (FC) and zero field cooled (ZFC) curves and Mössbauer spectroscopy. The results showed that dispersion in moderate quantities of paraffin significantly increases the crystallite size, the absolute value of the anisotropy field, the saturation magnetization and the blocking temperature of the nanoparticles, a result that may be of interest for practical applications of the composite.

1. Introduction

Nanometric manganese ferrite is a much-studied material for industrial and medical applications, such as microwave absorption, catalysis, magnetohyperthermia and drug delivery [1–4], due to its high saturation magnetization and good chemical stability [5]. However, due to magnetic attraction, ferrite nanoparticles tend to form agglomerates, which may compromise their performance for certain applications. One of the proposed solutions has been to disperse the nanoparticles in nonmagnetic materials [4–14]. A convenient nonmagnetic material is paraffin, a relatively cheap material with a low melting point.

The purpose of this work is to investigate the influence of dispersion in paraffin on the magnetic anisotropy of manganese ferrite. To achieve this end, we made samples with different dilutions of ferrite in paraffin.

2. Methods and results

2.1. Sample preparation

Manganese ferrite nanoparticles were synthesized by the combustion method [15]. Stoichiometric amounts of manganese nitrate, $Mn(NO_3)_2{\cdot}4H_2O$, Aldrich, 98%, and iron nitrate, $Fe(NO_3)_3{\cdot}9H_2O$, Aldrich, 98%, were dissolved in deionized

* *Corresponding author.*
E-mail: rsbiasi@ime.eb.br (R.S. Biasi).
https://doi.org/10.1016/j.jmrt.2017.09.010

Please cite this article in press as: Biasi RS, et al. Properties of manganese ferrite-paraffin composites. J Mater Res Technol. 2018. https://doi.org/10.1016/j.jmrt.2017.09.010

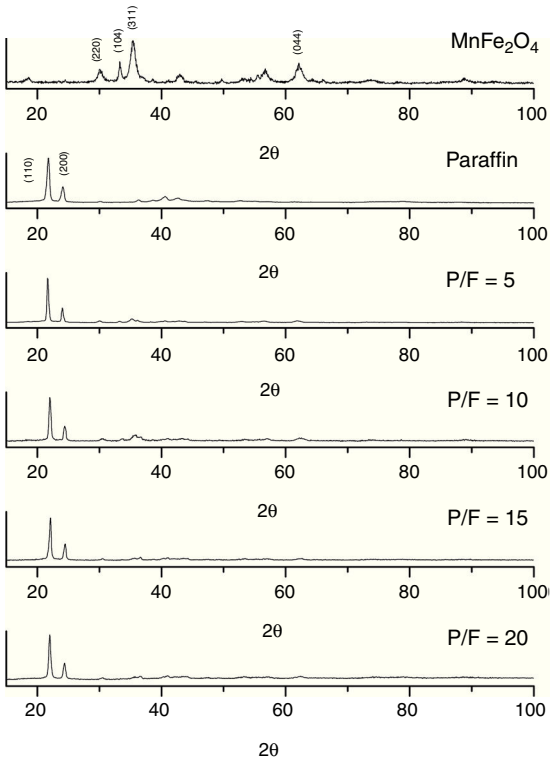

Fig. 1 – X-ray diffractograms of undiluted manganese ferrite, paraffin and manganese ferrite-paraffin composites.

water to obtain the starting solution. To this was added a solution of glycine, $C_2H_5NO_2$, Aldrich, 98.5%, with a glycine-nitrate molar ratio (G/N) of 0.5. The resulting solution was stirred for 20 min at room temperature and heated to 100 °C so that autocombustion would take place. The resulting ferrite powder was dispersed in molten paraffin with paraffin/ferrite weight (P/F) ratios of 5, 10, 15 and 20 using a 40 kHz ultrasonic bath.

2.2. *XRD measurements*

X-ray diffractograms were recorded at room temperature in a PANalytical X'Pert PRO diffractometer using Cu K_α radiation (0.15418 nm). Fig. 1 shows a diffractogram of undispersed ferrite powder, a diffractogram of paraffin, and diffractograms of P/F = 5, 10, 15 and 20 composites. A Rietveld refinement, performed using the HighScore plus 3.0 application, revealed that the sample of undispersed ferrite powder consists of 90% manganese ferrite ($MnFe_2O_4$), with an average crystallite size of 7 nm and a lattice constant of 0.85 nm, and 10% hematite (Fe_2O_3). The peaks labeled as (220), (311) and (440) are attributed to manganese ferrite, while the (401) peak is attributed to hematite. The files used in the analysis were ICSD-250539 for manganese ferrite and ICSD-415251 for hematite. The paraffin peaks (110) and (200) were identified using the file JCPDS 00-040-1995.

Since no ICSD file was available for paraffin, we could not perform a Rietveld refinement for the composites and thus, in this case, the lattice constant of the manganese ferrite

Table 1 – Diffraction angle 2θ of the (311) line, lattice constant a and average crystallite size d of undispersed powder (P/F = 0) and of manganese ferrite-paraffin composites.

P/F	2θ (degrees)	a (nm)	d (nm)
0	35.12	0.848	7
5	35.22	0.845	9
10	35.82	0.831	10
15	35.69	0.834	9
20	35.67	0.835	8

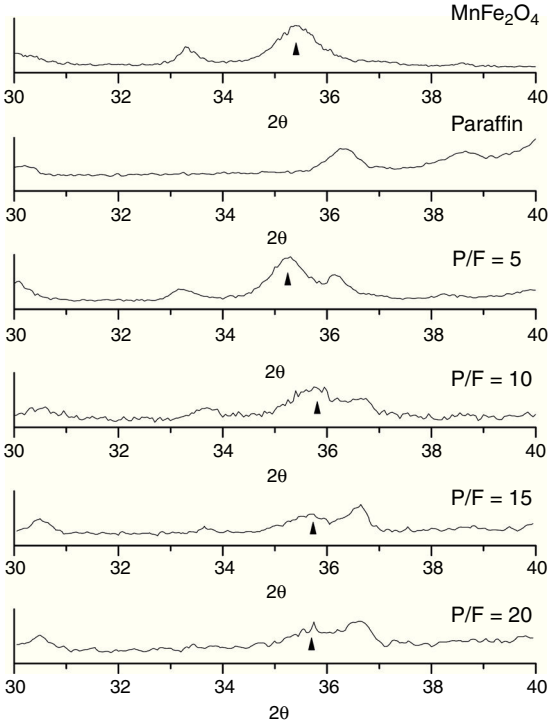

Fig. 2 – Expanded view of the (311) peak of manganese ferrite in the diffractograms of manganese ferrite-paraffin composites.

nanoparticles was determined using, for the (311) peak, the equation [16]

$$a = \frac{\lambda}{2 \cdot \sin\theta} \cdot \sqrt{h^2 + k^2 + l^2}, \quad (1)$$

where λ is the X-ray wavelength, θ is the diffraction angle and h, k and l are the Miller indices of the diffracting plane, and the average crystallite size was determined using, for the (311) peak, the Debye–Scherrer equation [16]

$$d = \frac{0.9\lambda}{B\cos\theta}. \quad (2)$$

where B is the peak width at half maximum. The results are shown in Table 1, where P/F = 0 means pure magnesium ferrite powder. Note that for pure manganese ferrite, the results were identical to those obtained using the Rietveld refinement.

An expanded view of the diffractograms is displayed in Fig. 2. The (311) peak of manganese ferrite, shown by an

Please cite this article in press as: Biasi RS, et al. Properties of manganese ferrite-paraffin composites. J Mater Res Technol. 2018. https://doi.org/10.1016/j.jmrt.2017.09.010

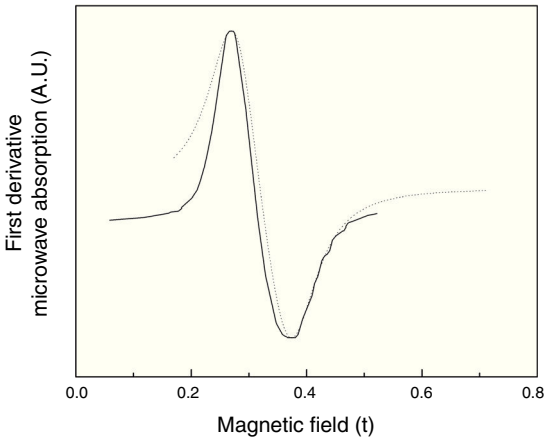

Fig. 3 – FMR spectrum of a manganese ferrite-paraffin composite with a paraffin-manganese ferrite weight ratio P/F = 5.

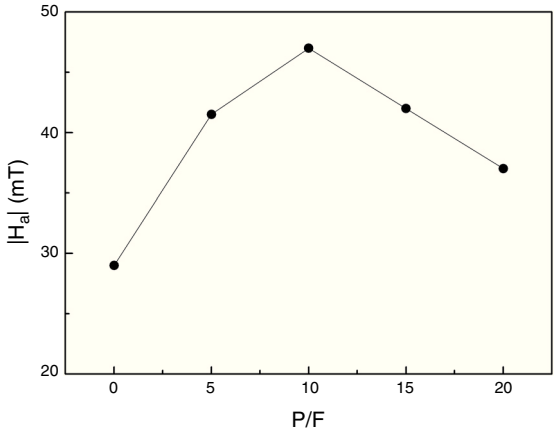

Fig. 4 – Dependence of the absolute value of the magnetic anisotropy of manganese ferrite-paraffin composites on the P/F ratio. The lines are only guides to the eye.

Table 2 – Magnetic resonance parameters of undispersed powder (P/F = 0) and of manganese ferrite-paraffin composites.

P/F	g	H_a (mT)	σ (mT)
0	2.10	−29.0	78.5
5	2.10	−41.5	90.3
10	2.10	−47.0	103.3
15	2.10	−42.0	97.9
20	2.10	−37.0	86.8

arrow, is shifted to the right in the composites and the maximum shift occurs for P/F = 10, while the peak of paraffin at $2\theta = 36.4^\circ$ is shifted to the left in the composites up to $2\theta = 36.8^\circ$ for P/F = 20. The reason for this behavior is discussed in Section 3.

2.3. *FMR measurements*

Ferromagnetic resonance measurements were performed at room temperature and 9.50 GHz using a Varian E-12 spectrometer with 100 kHz field modulation. The microwave power was 5 mW and the modulation amplitude was 1 mT. The magnetic field was calibrated with an NMR gaussmeter. Measurement of undiluted manganese ferrite powder was performed loading the powder in a quartz tube.

The experimental results were fitted to theoretical spectra using a computer program developed by Taylor and Bray [17] for paramagnetic resonance spectra and adapted by Griscom [18] for ferromagnetic resonance spectra. A typical spectrum is shown in Fig. 3 for a sample with P/F = 5. The fitting was generally good, except for the low field part of the spectra, where the slope of the amplitude rise is much steeper in the experimental curves. This mismatch is attributed [19] to superparamagnetic effects. The fitting parameters are shown in Table 2 and the dependence of the absolute value of the anisotropy field H_a on the P/F ratio is shown in Fig. 4.

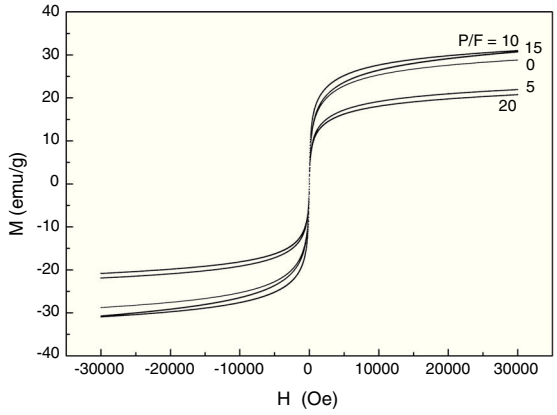

Fig. 5 – Hysteresis loops of all samples.

Table 3 – Saturation magnetization and blocking temperature of undispersed powder (P/F = 0) and of manganese ferrite-paraffin composites.

P/F	M (emu/g)	T_B (K)
0	28.8	<50
5	21.9	260
10	31.0	280
15	30.7	265
20	20.8	260

2.4. *Magnetization measurements*

Magnetization measurements were performed in an MPMS Quantum Design equipment using a Quantum Design VSM. The hysteresis loop at 300 K is shown in Fig. 5 and the FC and ZFC curves are shown in Fig. 6. The values of the saturation magnetization M at 300 K, obtained from the hysteresis loop, and of the blocking temperature T_B, obtained from the ZFC curves, are shown in Table 3. The blocking temperature of undiluted manganese ferrite could not be measured because the maximum of the ZFC curve is below 50 K and thus is out of the range of our equipment.

Please cite this article in press as: Biasi RS, et al. Properties of manganese ferrite-paraffin composites. J Mater Res Technol. 2018. https://doi.org/10.1016/j.jmrt.2017.09.010

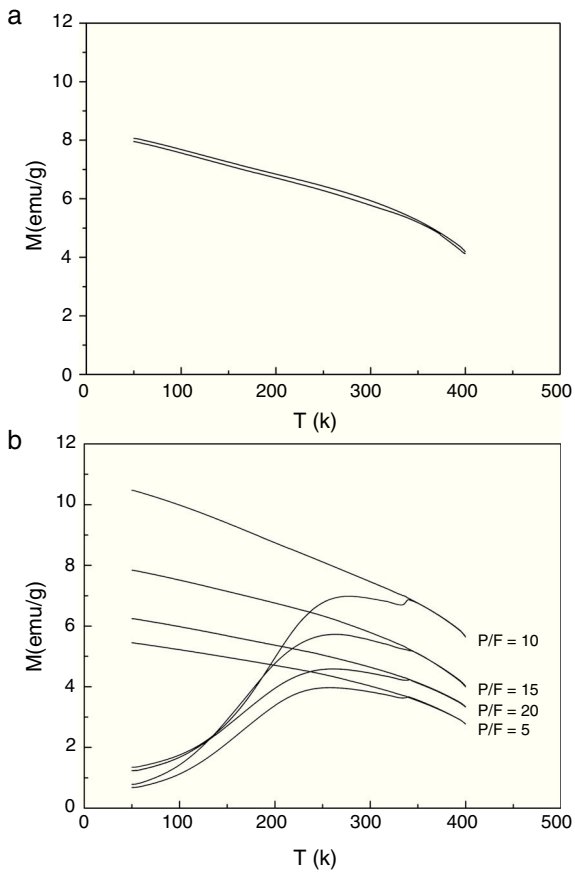

Fig. 6 – FC and ZFC curves (a) of undiluted manganese ferrite and (b) of manganese ferrite-paraffin composites.

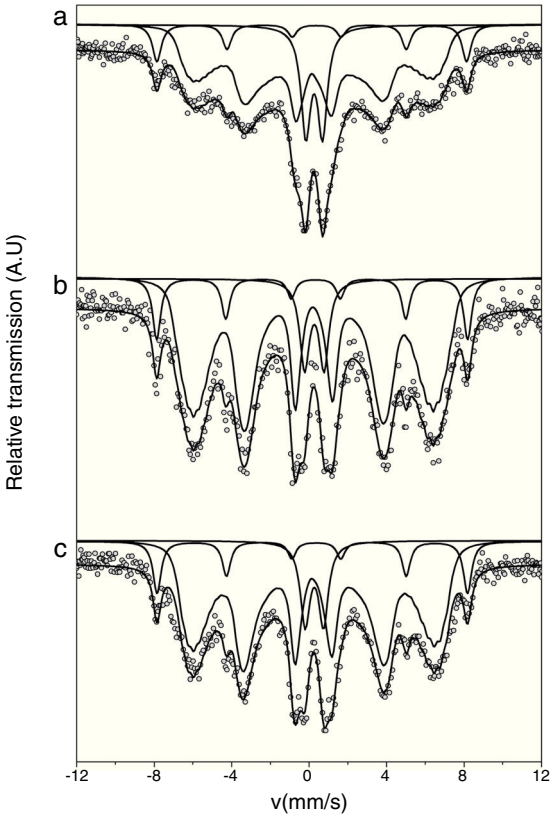

Fig. 7 – Mössbauer spectra of (a) undiluted manganese ferrite, (b) a manganese ferrite-paraffin composite with weight ratio P/F = 10 and (c) a manganese ferrite-paraffin composite with weight ratio P/F = 10.

Table 4 – Relative areas of the components of the Mössbauer spectra of undispersed ferrite powder (P/F = 0) and of manganese ferrite-paraffin composites.

P/F	S_1 (%)	S_2 (%)	D (%)
0	11	72	17
10	11	79	10
20	11	78	11

2.5. *Mössbauer measurements*

The Mössbauer spectra were recorded at room temperature in a homemade equipment of the Centro Brasileiro de Pesquisas Físicas (CBPF). Fig. 7 shows the Mössbauer spectra (a) of undispersed ferrite powder, (b) of the composite with P/F = 10 and (c) of the composite with P/F = 20. As shown in the figure, the spectra consist of three lines: a high amplitude sextet, a low amplitude sextet and a doublet. The low amplitude sextet is attributed to hematite, the high amplitude sextet to blocked ferrite particles in tetrahedral and octahedral sites (at room temperature, the sextets due to iron atoms in tetrahedral and octahedral sites are so wide that they cannot be separated) and the doublet is attributed to unblocked ferrite particles, i.e., particles in the superparamagnetic state. Table 4 shows the relative areas of the low intensity sextet (S_1), of the high intensity sextet (S_2) and of the doublet (D).

3. Discussion

The fact that parameters of the ferrite nanoparticles such as the anisotropy field (Table 2), the blocking temperature of superparamagnetism (Table 3) and the relative area of the Mössbauer sextet (Table 4) go through a maximum for P/F = 10 is coherent with the fact that the average size of the nanoparticles increases with increasing dilution for P/F < 10 and decreases with increasing dilution for P/F > 10 (Table 1). A faster saturation of the magnetization of manganese ferrite nanoparticles diluted with paraffin as compared with undiluted nanoparticles was observed by Aslibeiki and Kameli [5] and attributed to the interaction of paraffin with a disordered layer in the surface of the nanoparticles, making it more ordered and thus increasing the effective particle size. This is consistent with the fact that the (311) peak of the diffraction pattern of manganese ferrite is shifted to the right in all composites (Table 1 and Fig. 2), indicating a compressive tension exerted by the paraffin. On the other hand, the shift to the right of the paraffin peak suggests a tractive force, possibly due to the ultrasonic bath.

The decrease of the particle size for values of P/F larger than 10 appears to be related to the fact that the compressive tension exerted by the paraffin molecules decreases at high dilutions, as suggested by the increase in the lattice

Please cite this article in press as: Biasi RS, et al. Properties of manganese ferrite-paraffin composites. J Mater Res Technol. 2018. https://doi.org/10.1016/j.jmrt.2017.09.010

constant (see Table 1). The decrease of saturation magnetization for P/F > 10 is attributed to superparamagnetic effects, as evidenced by a decrease of the blocking temperature (see Table 3) and an increase of the relative number of unblocked particles observed in the Mössbauer spectra (see Table 4).

4. Conclusions

In this work, the properties of manganese ferrite nanoparticle-paraffin composites were investigated. The results showed that many measured parameters go through an extremum for P/F = 10. In particular, the saturation magnetization, the absolute value of the anisotropy field and the blocking temperature are maximum for this value of P/F, a finding that could be of interest for technological applications such as microwave absorption and drug delivery.

Conflicts of interest

The authors declare no conflicts of interest.

Acknowledgments

The authors thank CAPES and CNPq for financial help.

REFERENCES

[1] Deraz NM, Alarifi A. Controlled synthesis. Physicochemical and magnetic properties of nano-crystalline Mn ferrite system. Int J Electrochem Soc 2012;7:5534–43.
[2] Carta D, Casula MF, Floris P, Falqui A, Mountjoy G, Boni A, et al. Synthesis and microstructure of manganese ferrite coloidal nanocrystals. J Phys Chem Chem Phys 2010;12:5074–83.
[3] Kanagesan S, Aziz SBA, Hashim M, Ismail I, Tamilselvan S, Alitheen NBBM, et al. Synthesis characterization and in vitro evaluation of manganese ferrite ($MnFe_2O_4$) nanoparticles for their biocompatibility with murine breast cancer cells (4T1). Molecules 2016;21(312), 9 pp.
[4] Han Z, Li D, Liu X, Geng D, Li J, Zhang Z. Microwave-absorption properties of F(Mn) ferrite nanocapsules. J Phys D Appl Phys 2009;055008, 5 pp.
[5] Aslibeiki B, Kameli P. Magnetic properties of $MnFe_2O_4$ nano-aggregates dispersed in paraffin wax. J Magn Magn Mater 2015;385:308–12.
[6] Stejskal J, Trchová M, Brodinová J, Kalenda P, Fedorova SV, Prokeš J, et al. Coating of zinc ferrite particles with a conducting polymer, polyaniline. J Colloid Interface Sci 2006;298:87–93.
[7] Li BW, Shen Y, Yue ZX, Nan CW. Influence of particle size on electromagnetic behavior and microwave absorption properties of Z-type Ba-ferrite/polymer composites. J Magn Magn Mater 2007;313:322–8.
[8] Dosoudil R, Usáková M, Franek J, Grusková A, Sláma J. Dispersion of complex permeability and EM-wave absorbing characteristics of polymer-based composites with dual ferrite filler. J Magn Magn Mater 2008;320:e849–52.
[9] Shimba K, Tezuka N, Sugimoto S. Magnetic and microwave absorption properties of polymer composites with amorphous Fe–B/Ni–Zn ferrite nanoparticles. Mater Sci Eng B 2012;177:251–6.
[10] Malana MA, Qurexhi RB, Ashiq MN. Adsorption studies of arsenic on nano aluminium doped manganese copper ferrite polymer (MA, VA AA) composite: kinetics and mechanism. Chem Eng J 2011;172:721–7.
[11] Bayrakdar H. Complex permittivity, complex permeability and microwave absorption properties of ferrite–paraffin polymer composites. J Magn Magn Mater 2011;323:1882–5.
[12] Hayashi K, Maeda K, Moriya M, Sakamoto W, Yogo T. *In situ* synthesis of cobalt ferrite nanoparticle/polymer hybrid from a mixed Fe–Co methacrylate for magnetic hyperthermia. J Magn Magn Mater 2012;324:3158–64.
[13] Borah S, Bhattacharyya NS. Broadband magneto-dielectric response of particulate ferrite polymer composite at microwave frequencies. Compos Part B 2012;43:1988–94.
[14] Tong S-Y, Tung M-J, Ko W-S, Huang Y-T, Wang Y-P, Wang L-C, et al. Effect of Ni fillers on microwave absorption and effective permeability of NiCuZn ferrite/Ni/polymer functional composites. J Alloys Compd 2013;550:39–45.
[15] Aruna ST, Mukasyan AS. Combustion synthesis and nanomaterials. Curr Opin Solid State Mater Sci 2008;12:44–50.
[16] Cullity BD. Elements of X-ray diffraction. 2nd ed. Reading, MA: Addison-Wesley; 1978.
[17] Taylor PC, Bray PJ. Computer simulations of magnetic resonance spectra observed in polycrystalline and glassy samples. J Magn Reson 1970;2:305–31.
[18] Griscom DL. Ferromagnetic resonance of precipitated phases in natural glasses. J Non-Crystalline Solids 1984;67:81–118.
[19] de Biasi RS, Lopes RDS, Carvalho DG, Figueiredo ABS. FMR lineshape of cobalt ferrite nanoparticles. Ceram Int 2015;41:865–7.

Please cite this article in press as: Biasi RS, et al. Properties of manganese ferrite-paraffin composites. J Mater Res Technol. 2018. https://doi.org/10.1016/j.jmrt.2017.09.010